Final Draft
of the original manuscript:

Enz, J.; Khomenko, V.; Riekehr, S.; Ventzke, V.; Huber, N.; Kashaev, N.:
Single-sided laser beam welding of a dissimilar AA2024–AA7050 T-joint
In: Materials and Design (2015) Elsevier

DOI: 10.1016/j.matdes.2015.03.049

Single-sided laser beam welding of a dissimilar AA2024-AA7050 T-joint

Authors: J. Enz, V. Khomenko, S. Riekehr, V. Ventzke, N. Huber, N. Kashaev

Affiliation: Helmholtz-Zentrum Geesthacht, Institute of Materials Research, Materials Mechanics, Max-Planck-Straße 1, 21052 Geesthacht, Germany

Corresponding author: J. Enz, Tel.: +49-4152-87-2507, Fax: +49-4152-87-42507, E-mail: josephin.enz@hzg.de

Abstract

In the aircraft industry double-sided laser beam welding of skin-stringer joints is an approved method for producing defect-free welds. But due to limited accessibility - as for the welding of skin-clip joints - the applicability of this method is limited. Therefore single-sided laser beam welding of T-joints becomes necessary. This also implies a reduction of the manufacturing effort. However, the main obstacle for the use of single-sided welding of T-joints is the occurrence of weld defects. An additional complexity represents the combination of dissimilar and hard-to-weld aluminium alloys - like Al-Cu and Al-Zn alloys. These alloys offer a high strength-to-density ratio, but are also associated with distinct weldability problems especially for fusion welding techniques like laser beam welding. The present study demonstrates how to overcome the weldability problems during single-sided laser beam welding of a dissimilar T-joint made of AA2024 and AA7050. For this purpose a high-power fibre laser with a large beam diameter is used. Important welding parameters are identified and adjusted for achieving defect-free welds. The obtained joints are compared to double-sided welded joints made of typical aircraft aluminium alloys. In this regard single-sided welded joints showed the expected differing weld seam appearance, but comparable mechanical properties.

Keywords: single-sided laser beam welding; T-joint; Al-Cu alloy; AA2024; Al-Zn alloy; AA7050

Introduction

AA2xxx and AA7xxx series alloys - like AA2024 and AA7050 - are age-hardenable aluminium alloys which have been widely used in the aircraft industry for many years due to their high strength-to-density ratio and machinability as well as their easy availability. But these alloys are often associated with distinct weldability problems - such as the formation of porosity and hot cracking - especially for fusion welding techniques like laser beam welding (LBW) [1-3]. The porosity mostly arises from the evaporation of the volatile elements zinc and magnesium - the main alloying elements of AA7xxx series alloys - and from the resulting instabilities of the narrow keyhole during LBW [2].

Double-sided LBW - simultaneous or successive - is an approved method for joining skin-stringer T-joints in the aircraft industry since symmetrical and defect-free weld seams can be achieved (see Fig. 1) [4-7].

Due to limited accessibility - for example for the welding of skin-clip T-joints - single-sided LBW may become necessary. Furthermore, the manufacturing efforts for skin-stringer joints could also be reduced by single-pass welding with just one laser beam. However this welding method generally results in an increased porosity at the root side of the weld seam and insufficient or excessive penetration as shown in

preliminary internal studies (see Fig. 2a and b). The work of the European Project ‘Wel-Air’ and Ventzke et al. showed that the reason for this is the unfavourable degassing condition during single-sided welding [8,9]. The aluminium clip represents a cooling trap - due to the high thermal diffusivity of aluminium - which yields in a faster cooling and hence in a faster solidification of the melt at the root side of the weld. By this means, pores can be easily entrapped within the melt and angular distortion can occur [9,10]. The non-uniform temperature distribution during single-sided welding of T-joints was disclosed by Shanmugam et al. and Machold et al. [11,12]. In contrast to that the double-sided laser welding shows a symmetrical temperature distribution and hence a considerable reduced tendency for porosity formation and angular distortion [10].

In previous studies it was also demonstrated that an incident beam angle between 10° and 15° (Oliveira et al.) or lower than 25° (Ventzke et al.) showed a reduction of porosity due to the opening of the keyhole at the root side of the weld in connection with an equalization of temperature [9,13]. However, it was impossible to completely eliminate the weld porosity. The work of Leong et al. showed that an increased beam diameter has a beneficial effect on the laser weldability of a material due to reduced beam irradiance [14]. The beam irradiance is defined as the relation of laser beam power to the area of laser interaction. In addition, the resulting enlarged keyhole enables a better degassing especially at the root side of the weld seam. An enlargement of the laser beam by the change of focal position - beyond the Rayleigh length - is often accompanied by a reduced power density and shielding of the laser beam by plasma. For this reason it is not recommended to realize large beam diameters just by the change of the focal position. Hence, it can be concluded that a laser source with an initially large beam diameter and a high beam quality - facilitating a high Rayleigh length - has to be used instead. The laser beam diameter is defined by the fibre diameter and the used optical system. The quality of a laser beam is quantified by the beam parameter product (BPP). Another advantage of an enlarged laser beam and a high Rayleigh length is the increased positional tolerance. This means, that slight changes of the position are easily compensated. For assuring a full penetration in spite of the large beam diameter a high-power laser source is needed. A potential laser source which offers high beam qualities in combination with high laser beam power is the fibre laser [15].

The present study shows how to overcome the weldability problems during single-sided LBW of dissimilar T-joints made of AA2024 and AA7050. For this purpose a high-power fibre laser with an enlarged laser beam diameter was used and the welding process was optimized in particular by the adjustment of the incident beam angle and position.

Materials and experimental methods

The T-joint consists of two dissimilar aluminium alloys. The Al-Cu-Mg alloy AA2024 in T3 temper condition and with a two-sided Al cladding is used as skin alloy. The skin sheet has a thickness of 2.0mm. The Al-Zn-Cu-Mg alloy AA7050 in T76 temper condition is used as stringer material. The I-shaped stringer or clip has a thickness of 2.0mm. Due to the choice of alloy and temper condition the stringer material possesses a higher strength than the skin material. This aspect is essential for the stiffening of the final fuselage structure. Since the age-hardenable aluminium alloys tend to develop metallurgical induced cracks in the weld seam, the T-joint has to be welded with an additional filler wire which has a high Si-content to avoid the crack

formation. In this study the Al-Si alloy AA4047 is used as filler wire with a diameter of 1.2mm. The high silicon content in combination with a low magnesium and copper content of this alloy supports the prevention of hot cracks during welding [2]. The chemical composition of the used aluminium alloys are shown in Table 1. Before welding the oxide layer was removed in the joining zone of skin and stringer by mechanical grinding, in order to avoid its unfavourable influence on the weld seam quality.

The single-sided LBW of the T-joint was performed using a 6-axis industrial robot which was connected to an 8.0kW fibre laser. The laser fibre had a diameter of 300µm and the used optic had a focal length of 300mm. The beam caustic was measured using a PRIMES Focus Monitor. The laser beam diameter in focus position was 746µm and the confocal parameter (twice the Rayleigh length) was approximately 24.6mm as shown in Fig. 3a. The measured BPP of the used laser beam was 11.3. The beam possessed a top-hat profile near to the focus position, but with increasing defocussing it altered to a more Gaussian-like profile as shown in Fig. 3b and c. The top-hat profile provides a large area of constant irradiance, which is needed for retaining a keyhole with a large diameter.

For retaining the position of the skin and the stringer during welding a mechanical clamping device was used. The filler wire was supplied by a dragging wire feed. Helium gas was used as shielding gas. The advantages of Helium in comparison to Argon as shielding gas for welding aluminium alloys are on the one hand the higher heat input into the material which enables higher welding speeds for the same penetration depth. On the other hand it is the lower tendency to form porosity due to the higher temperatures and the lower viscosity of the melt pool which allows better degassing. The shielding gas was supplied from front and root side of the weld in order to provide a complete shielding of the melt pool. The used welding configuration is shown in Fig. 4. The optimized laser welding process - with respect to weld seam appearance and porosity - was obtained by the variation of the following parameters:

- laser beam power (3.5kW - 8kW),
- incident beam angle (13° - 17°),
- incident beam position (0mm - 0.5mm),
- focal position (+0mm - +8mm),
- welding speed (2m/min - 8m/min) and
- filler wire feed rate (2m/min - 8m/min).

For the purpose of comparison successive LBW was additionally performed. Therefore the same laser and welding configuration was used as for the single-sided LBW. After the first welding trail the specimen was turned and the second welding trail was conducted. This resulted in an inverse orientation of the direction of welding. For the successive LBW a lower laser beam power was necessary, since only a partial penetration of the stringer/clip is required for each welding trail. But the particular penetration depth had to be sufficient for achieving an overlapping of both weld seams and hence a complete connection of the stringer/clip to the skin.

Visual inspection was used to determine the outer appearance of the weld seam, especially for weld imperfections such as incomplete filled grooves and undercutting of the weld seam. In contrast to that, X-ray inspection was used to determine inner

imperfections such as porosity and cracks. The microstructural properties of the joints were investigated by optical microscopy.

The mechanical properties of the joints were determined by the use of Vickers micro-hardness testing (HV 0.2). Therefore several indentations were made at all regions of the joint - fusion zone, heat affected zone and both base materials of skin and stringer/clip. Pull-out tests of the welded T-joints were performed in order to assess the weld seam quality and the connection of the stringer to the skin. Therefore, load is applied on the stringer/clip in perpendicular direction to the skin. This type of test does not represent a real load case of an aircraft skin-stringer structure, but it is a simple way to compare the joint strength of different welds. Hoop-stress tests were also performed on the welded T-joints by applying a load on the skin in perpendicular direction to the stringer. Here, the test represents the load condition in the skin of a pressurized fuselage. In addition the joint efficiency can be determined with the help of the hoop-stress results. Therefore the results of the welded joints are compared to the result of the base material. All obtained results were compared to double-sided welded T-joints made of typical aircraft aluminium alloys as described in [4].

Results and discussion

The single-sided LBW of the T-joints always resulted in an asymmetric shape of the weld seam. The front side of the weld shows a concave shape whereas the root side of the weld shows a slight convex shape. This asymmetry is mandatory since no symmetric welding setup was used. But by variation of the welding parameters it was possible to influence the weld seam shape and quality within certain limits.

Influence of the beam diameter and defocussing

The large initial beam diameter of 746µm used in this study led to a significant reduction of porosity in the weld seam in comparison to welded joints with smaller beam diameters, but also to an increase of the weld seam size. The defocussing of the laser beam within the Rayleigh length led only to a slight increase of the beam diameter. However, by defocussing in positive direction (away from the surface), it was possible to adjust the shape and size opening of the keyhole at front and root side of the weld seam. As a consequence of increasing defocussing the irradiance distribution changes from a top-hat profile to a more and more Gaussian profile. This limits the degree of defocussing as mentioned earlier.

Influence of the laser beam power, welding speed and filler wire feed rate

By the adjustment of laser beam power and welding speed it was possible to achieve an adequate penetration of the T-joint region between skin and stringer/clip. In comparison to the welding with smaller beam diameters, an enlarged beam diameter will always need higher power levels in order to achieve the same beam irradiances and hence the same penetration levels. This means that by doubling the beam diameter an approximately four times higher laser beam power is required as shown in Fig. 5. A high laser beam power is also required in order to realize the welding with an enlarged beam diameter and also higher welding speeds. Besides, low welding speeds led to an increase of porosity in the weld seam due to the temperature increase and the resulting vaporisation of elements. The adjustment of the filler wire feed rate allowed a reduction of the convexity and also the undercut at the front side of the weld seam to a certain extent. Further increase of the feed rate led only to an

excess of weld metal at the root side of the weld, but not to a change of the shape of the front side.

Influence of the incident beam angle and position

By the adjustment of the incident beam angle and position it was possible to reduce the penetration into the skin to a minimum, to reduce the porosity and to improve the shape of the weld seam. An enhanced symmetry also supports prevention of angular distortion of the T-joint. The lower limit of the incident beam angle was defined by the geometry of the welding setup and excessive melting of the skin in front of weld seam, whereas the upper limit was defined by the occurrence of weld porosity due to the unfavourable temperature distribution. The optimal incident beam position is defined by the minimal achievable penetration into the skin with an adequate connection of the stringer to the skin. Thus the influence on the mechanical properties of the skin material is minimized. The required offset of the beam into the stringer strongly depends on the beam diameter and the used welding parameters. This means that for larger beam diameters and a higher heat input the offset into the stringer material has to be larger.

Optimized welding parameters

With the help of the obtained knowledge from the parameter study, it was possible to determine the optimal welding parameter set for single-sided and successive LBW of the T-joints, as summarized in Table 2. These welding parameters were used to produce the T-joint specimens for the investigations carried out in this study.

Results of the visual inspection

At the front side of the weld seams - especially in case of the single-sided welded joint - a dark deposit was observed. These fine particles originated from the evaporation of the alloying elements during welding and condensed mainly on the skin surface due to the low incident beam angle used for the welding of the T-joints. The deposit could be wiped away easily and no burning or melting of the skin occurred. In Fig. 6a some of the remaining dark deposit can be seen. Only at the root side of the single-sided weld seam a few tiny spatter marks were observed, as shown in Fig. 6b. The surfaces of both welded joints showed a regular and smooth surface.

Results of the X-ray inspection

The radiograph of the optimized single-sided T-joint is shown in Fig. 7a. It showed no porosity at all. In addition the evenness of the weld seam can be seen easily. In contrast to that, the successively welded T-joints showed a distinct porosity in the centre of the weld seam (see Fig. 7b) although a lower laser beam power level was used for welding which should result in a decreased vaporization tendency of volatile elements. This contradictory behaviour can be explained by the unfavourable degassing behaviour in the partially penetrated keyhole as well as the inhomogeneous temperature distribution in the weld which led to a faster solidification of the melt.

Results of the metallographic inspection

The weld seam area of the single-sided welded joint is significantly larger than the successively welded joint (see Fig. 8a and b) as well as for common simultaneously

welded joints (see also Fig. 1). This is mainly due to the larger beam diameter and the higher laser beam power which is necessary to achieve defect-free welds.

In addition, the single-sided welded joints showed a certain asymmetry due to the used welding configuration. In this regard the front side of the weld seam is characterized by concavity whereas the root side of the weld seam showed a more convex shape. The successively welded joints showed a higher symmetry and a similar seam angle, but in the centre of the resulting weld seam a reduced cross-section area was observed which could act as a metallurgical notch in combination with the area of overlapping of the single weld seams.

The maximum penetration depth of the single-sided weld was approximately 0.48mm which is 24% of the total skin thickness. Simultaneously welded joints always show higher penetration depth. Only for the successively welded joints a lower penetration depth into the skin of 0.22mm (11%) can be achieved. This is due to the single-sided welding mode and the lower power needed which results in a reduction of the melt pool.

The single-sided welded T-joint showed a very good dilution of the fed filler wire especially in comparison to the double-sided welded joints (see Fig. 1 and 8a). The reason for this could be the differing size and orientation of the keyhole and the resulting changes in the fluid flow in the melt pool.

Results of mechanical properties

The results of the microhardness tests for the single-sided welded T-joint are shown in Fig. 9. The obtained values are compared with a T-joint successively welded and T-joints welded simultaneously from both sides of the stringer [4]. It can be seen, that the size of the single-sided weld is larger, but the hardness level is only slightly below the values of the successively welded joint. This difference can be explained by the different heat input for both welds. For the single-sided welding a high heat input is necessary in order to achieve defect-free welds. In this context it should be also mentioned that the apparently smaller weld seam of the successively welded joint can only be found in the centre of the weld seam. The outer areas of the resulting weld seam showed a similar width as for the single-sided welded joint, as it can be seen in Figure 8b.

The results of the hoop-stress tests are shown in Fig. 10 and in Table 3. The higher joint efficiency of the single-sided welded joint - with approximately 90% of the ultimate tensile strength (UTS) of the base material - can be explained by the very low weld penetration into the skin material, which results in a reduced weakening of the skin material due to local dissolution of precipitation hardening [9]. Furthermore the occurrence of porosity and the area of overlapping in the resulting weld seam of the successively welded joint are expected to lead to an earlier failure of the joint. The fracture strain (A_f) of the single-sided welded joint was also slightly higher as for the double-sided welded joints.

In both joint types the failure initiates at the fusion boundary of the weld seam at the surface of the skin material and propagates through the thickness in a certain angle as shown in Figure 11. But there was no further propagation along the fusion boundary observed as for the simultaneously welded T-joints [4,6,7]. Also no preferential side - front or root of the weld seam - for crack initiation could be

identified. In addition, both joint types showed necking of the skin material before the final failure occurs.

In Fig. 12 the results of the pull-out tests are shown. The single-sided welded T-joint shows comparable results to the simultaneously welded joints made of typical aircraft aluminium alloys. Only the AA2198T3-AA2198T3 joint shows better results for the maximum achievable stress and displacement. The weak performance of the AA2198T3-AA2196T8 joint can be explained by the often inferior weld seam quality in matters of residual porosity and hot cracks as well as the insufficient dilution of the base material and filler material, compare also with Fig.1 and [4]. But since this test serves as a tool for the estimation of the weld seam quality, a sufficient connection of the stringer to the skin can be expected. The large weld seam area of the single-sided welded joints showed no disadvantageous effect on the results of the pull-out test.

The failure of the pull-out specimens occurred in both cases at the fusion boundary of the stringer material, since this is the location with the smallest cross-section area in load direction (see Fig. 13). Due to the low sheet thickness and the resulting high deformation of the skin sheet during testing another crack was observed starting within the weld metal. But this crack never led to the complete failure of the specimen, because of the prior failure along the fusion boundary.

Conclusions

On the basis of the obtained results of this study the following conclusions can be drawn:

(1) The single-sided LBW of porosity-free T-joints was accomplished by the use of a high power fibre laser with an enlarged beam diameter (compared to the commonly used LBW technique) and the adjusting of the welding parameters. In comparison to that, the successively welded T-joints showed a significant higher porosity. This can be explained by the improved degassing condition for single-sided welding due the enlarged keyhole and the homogeneous temperature distribution in the melt.
(2) The single-sided welded T-joints showed a larger weld seam area as the double-sided welded T-joint due to the high laser beam power and the large beam diameter used for welding. However, it was possible to reduce the penetration into the skin material by adjusting the incident beam angle and position.
(3) The mechanical properties of the single-sided welded T-joints are comparable to the results of double-sided welded T-joints of common aircraft aluminium alloys. The microhardness in the fusion zone is only slightly lower as for the successively welded joint. The joint efficiency of the single-sided joints is higher as for the double-sided welded joints. This is due to the reduced heat input and penetration into the skin material. The results of the pull-out test are comparable to most of the double-sided welded joints made of other aircraft aluminium alloys.

References

[1] C.M. Allen: ‘Laser welding of aluminium alloys - principles and applications’, TWI Report 759, 2004.

[2] J.C. Ion: ‘Laser beam welding of wrought aluminium alloys’, Science and Technology of Welding & Joining, Vol. 5 (5), 2000, pp. 265-276. http://dx.doi.org/10.1179/136217100101538308

[3] F. Palm: ‘Residual strength in integral (welded) Al fuselage structures - Understanding failure peculiarities enables amazing strength values’, Proc. Int. Conf. on Trends in Welding Research, Pine Mountain, USA, 2005.

[4] J. Enz: ‘Laser beam welding of high-strength aluminium-lithium alloys’, HZG Report 2012-2, 2012.

[5] J. Enz, S. Riekehr, V. Ventzke, N. Kashaev, N. Huber: ‘Process optimisation for the laser beam welding of high-strength aluminium-lithium alloys’, Schweißen und Schneiden, Vol. 64 (8), 2012, pp. 482-485.

[6] A. Prisco, F. Acerra, A. Squillace, G. Giorleo, C. Pirozzo, U. Prisco et al.: ‘LBW of similar and dissimilar skin-stringer joints. Part 1: Process optimization and mechanical characterization’, Advanced Materials Research, 2008. http://dx.doi.org/10.4028/www.scientific.net/AMR.38.306

[7] Z.B. Yang, W. Tao, L.Q. Li, Y.B. Chen, F.Z. Li, Y.L. Zhang: ‘Double-sided laser beam welded T-joints for aluminium aircraft fuselage panels: Process, microstructure, and mechanical properties’, Materials and Design, Vol. 33, 2012, pp. 652-658. http://dx.doi.org/10.1016/j.matdes.2011.07.059

[8] ‘WEL-AIR: Development of short distance welding concepts for airframes’, EU Project, 2007. http://ec.europa.eu/research/transport/projects/items/wel_air_en.htm, Accessed on 5 January 2015.

[9] V. Ventzke, S. Riekehr, M. Horstmann, P. Haack, N. Kashaev: ‘One-sided Nd:YAG laser beam welding for the manufacture of T-joints made of aluminium alloys for aircraft construction’, Welding and Cutting, Vol. 13 (4), 2014, pp. 245-249.

[10] X. Sun: ‘Knowledge modelling for the laser beam welding process in the aircraft industry’, MSc Thesis, Cranfield University, UK, 2011. http://dspace.lib.cranfield.ac.uk/handle/1826/7180

[11] N.S. Shanmugam, G. Buvanashekaran, K. Sankaranarayanasamy and S.R. Kumar: ‘A transient finite element simulation of the temperature and bead profiles of T-joint laser welds’, Materials & Design, Vol. 31 (9), 2010, pp. 4528-4542. http://dx.doi.org/10.1016/j.matdes.2010.03.057

[12] W. Machold, P. Staron. F. Bayraktar, S. Riekehr, M. Koçak and A. Schreyer: ‘Influence of the welding sequence on residual stresses in laser welded T-joints of an airframe aluminium alloy’, Materials Science Forum, Vol. 571, 2008. http://dx.doi.org/10.4028/www.scientific.net/MSF.571-572.375

[13] A.C. Oliveira, R.H.M. Siqueira, R. Riva and M.S.F. Lima: ‘One-sided laser beam welding of autogenous T-joints for 6013-T4 aluminium alloy’, Materials & Design, 2014. http://dx.doi.org/10.1016/j.matdes.2014.09.055

[14] K.H. Leong and H.K. Geyer: ‘Laser beam welding of any metal’, Proc. Int. Cong. on Applications of Lasers and Electro-Optics (ICALEO), Orlando, USA, Laser Institute of America, Vol. 8, 1998.

[15] R. Poprawe: ‘Lasertechnik für die Fertigung: Grundlagen, Perspektiven und Beispiele für den innovativen Ingenieur’, Springer Verlag, 2005, pp.147-160.

Figure captions:

Fig. 1: Typical macrographs of AA2198T3-AA2198T3 (a) and AA2198T3-AA2196T8 (b) joints simultaneously welded with a CO_2 laser [4].

Fig. 2: Macrographs of an AA6082-AA5083 joint single-sided welded with a Nd:YAG laser (BPP=14.5) and typical defects: insufficient penetration (a) and excess of penetration (in combination with porosity and undercut) (b).

Fig. 3: Measured dimensions of the used laser beam close to the focus position (a); schematic sketch of the measured irradiance distribution in the focus position (b) and beyond the Rayleigh length (c).

Fig. 4: Used configuration for the single-sided and successive LBW of T-joints.

Fig. 5: Influence of the beam diameter on the laser beam power required for achieving the same beam irradiance.

Fig. 6: Macrographs of the front (a) and the root side (b) of the optimized single-sided welded T-joint and the successive welded T-joint (c) and (d) (the arrow indicates the welding direction).

Fig. 7: Radiograph of the optimized single-sided welded T-joint (a) and successive welded T-joint with pores in the weld seam (b).

Fig. 8: Macrographs of the optimized single-sided welded T-joint (a) and the successively welded T-joint (b).

Fig. 9: Results for microhardness testing of the single-sided welded AA2024T351-AA7050T76 T-joint in comparison to different double-sided welded T-joints.

Fig. 10: Results for the hoop-stress testing of the single-sided welded AA2024T351-AA7050T76 T-joint in comparison to different double-sided welded T-joints.

Fig. 11: Locations of the fracture during hoop-stress testing in the single-sided welded (a) and the successively welded T-joint (b).

Fig. 12: Results for the pull-out testing of the single-sided welded AA2024T351-AA7050T76 T-joint in comparison to different double-sided welded T-joints (see also [4]).

Fig. 13: Locations of the fracture during hoop-stress testing in the single-sided welded (a) and the successively welded T-joint (b).

Table captions:

Tab. 1: Chemical composition of the used Al alloys.

Tab. 2: Optimized parameters for single-sided and successive LBW.

Tab. 3: Ultimate tensile strengths and fracture strains of the different welded joints (W) in comparison to the base material (BM) obtained from the hoop-stress test.

Figure 1

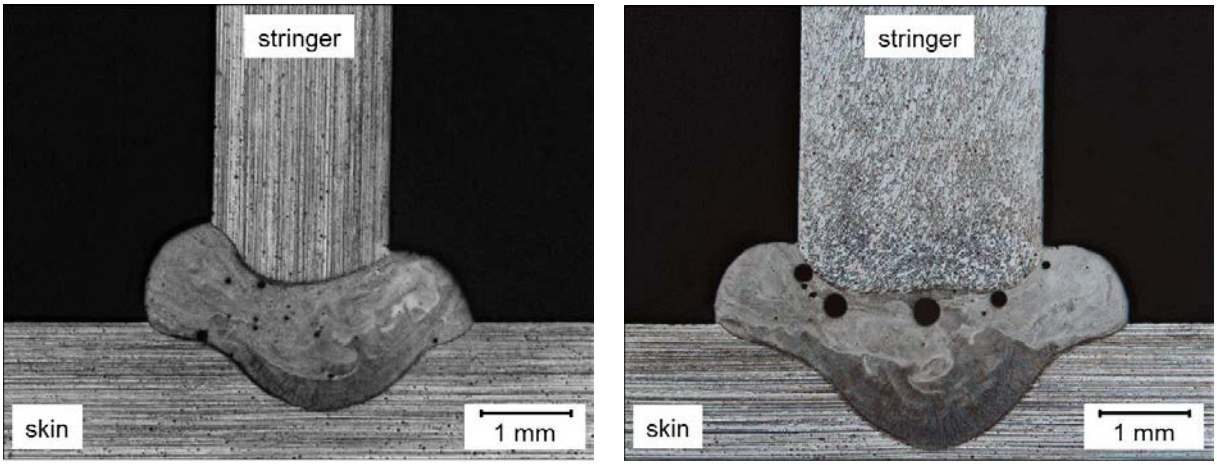

(a) (b)

Figure 2

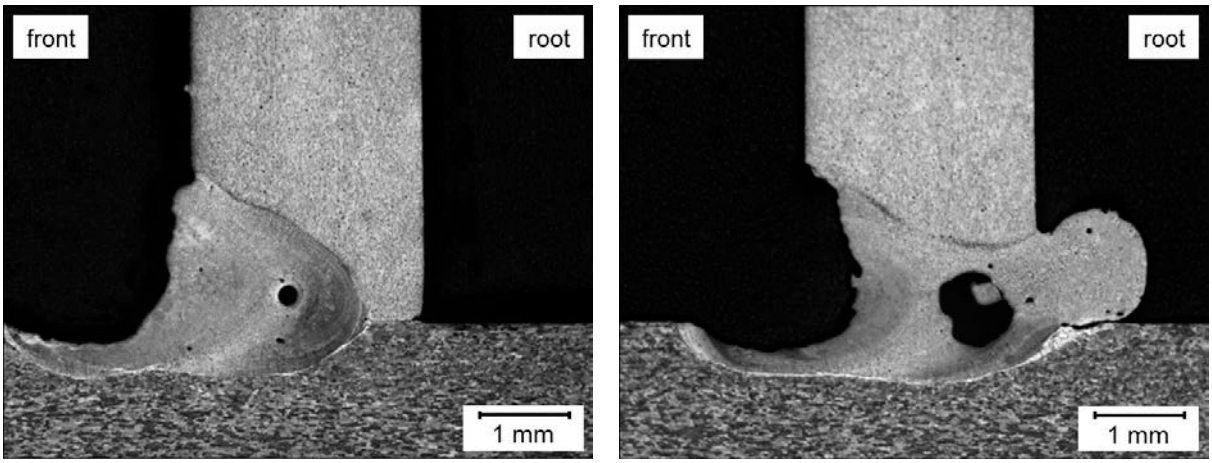

(a) (b)

Figure 3

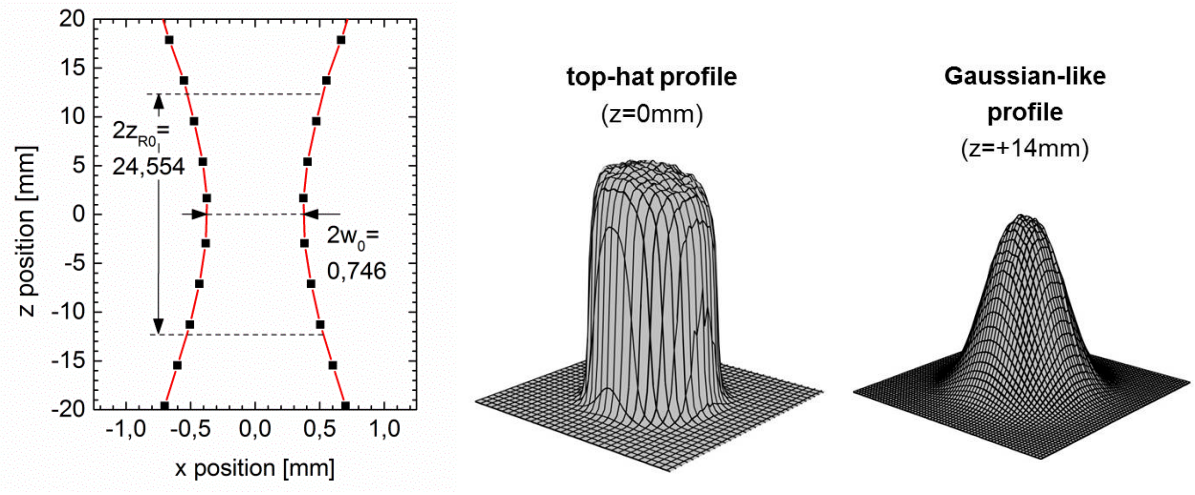
20
15
10
5
0
-5
-10
-15
-20
z position [mm]
-1,0
-0,5
0,0
0,5
1,0
x position [mm]
2z_R0 =
24,554
2w_0 =
0,746
top-hat profile
(z=0mm)
Gaussian-like
profile
(z=+14mm)

(a) (b) (c)

Figure 4

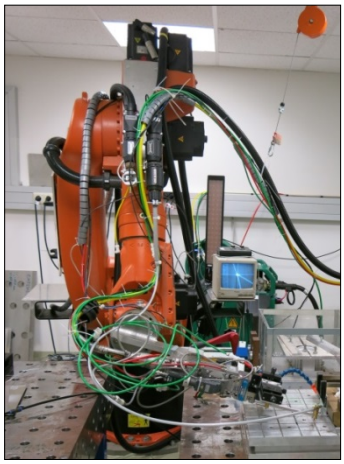

(a)

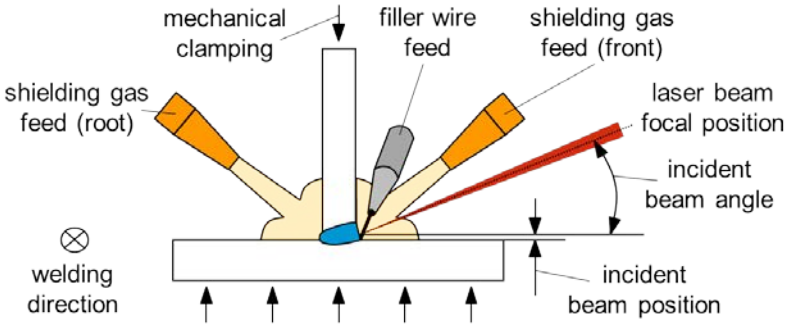
mechanical clamping
filler wire feed
shielding gas feed (front)
shielding gas feed (root)
laser beam focal position
incident beam angle
welding direction
incident beam position

(b)

Figure 5

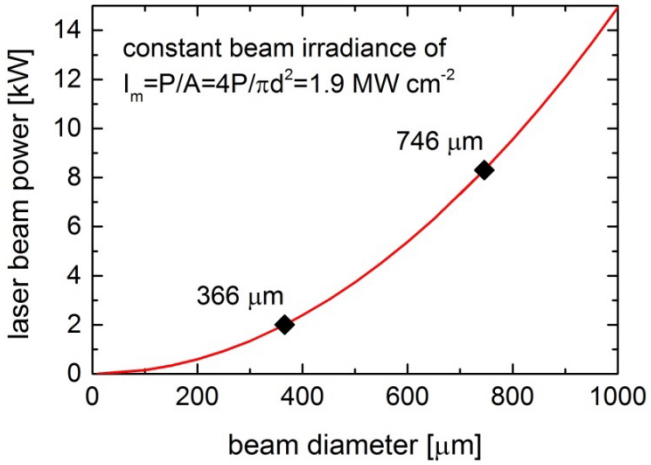
constant beam irradiance of
$I_m=P/A=4P/\pi d^2=1.9$ MW cm^{-2}
746 μm
366 μm
laser beam power [kW]
beam diameter [μm]
0
2
4
6
8
10
12
14
0
200
400
600
800
1000

Figure 6

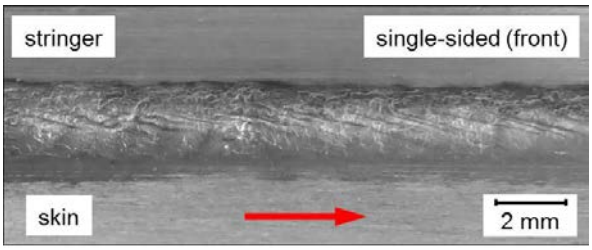

(a)

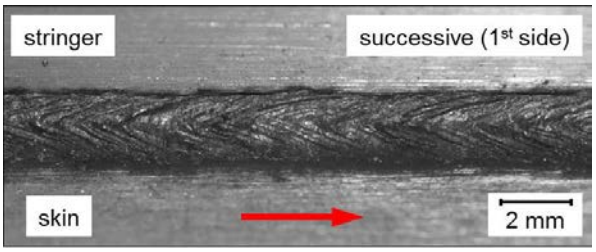

(c)

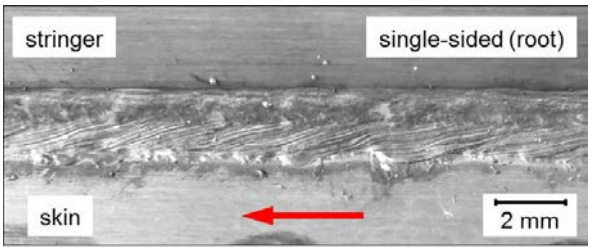

(b)

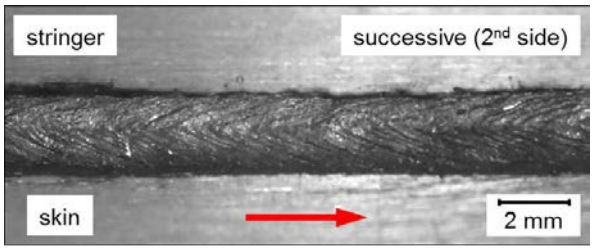

(d)

Figure 7

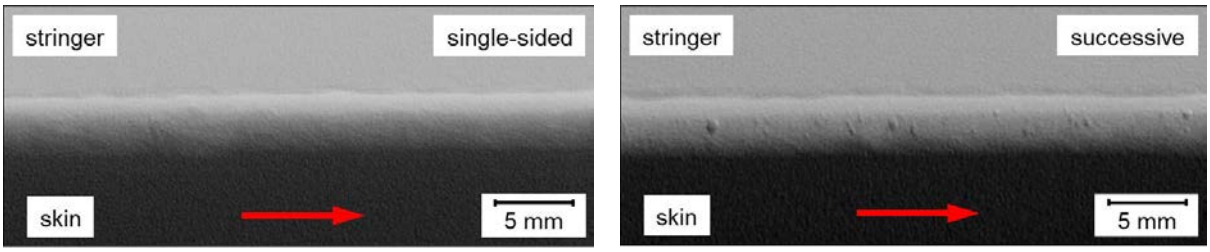
stringer
single-sided
skin
5 mm
stringer
successive
skin
5 mm

(a) (b)

Figure 8

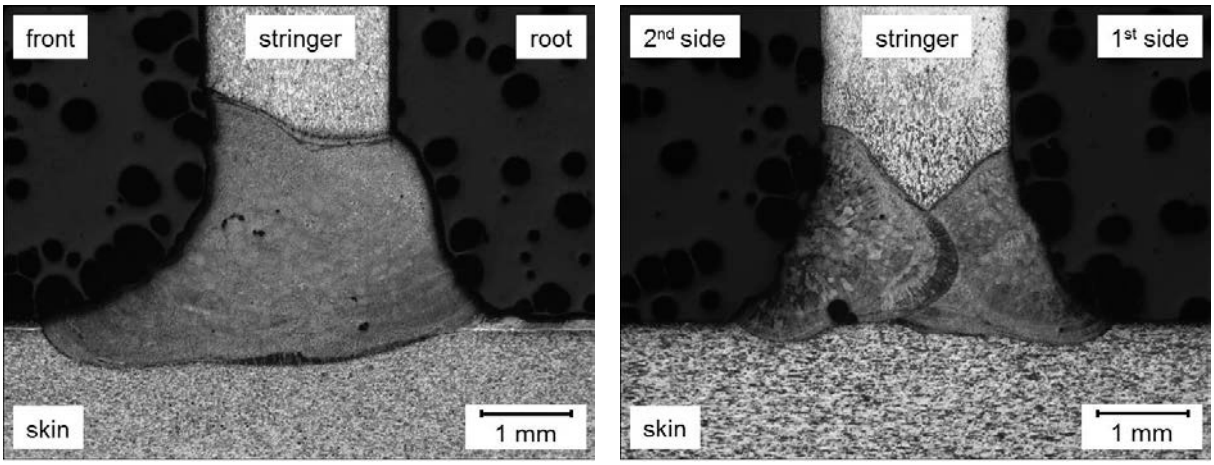
front
stringer
root
skin
1 mm
2nd side
stringer
1st side
skin
1 mm

(a) (b)

Figure 9

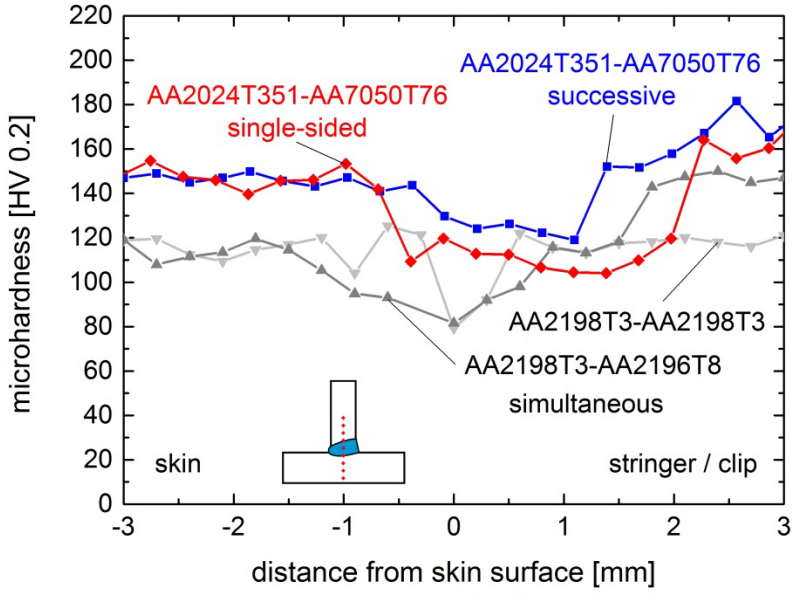
microhardness [HV 0.2]
distance from skin surface [mm]
AA2024T351-AA7050T76
single-sided
AA2024T351-AA7050T76
successive
AA2198T3-AA2198T3
AA2198T3-AA2196T8
simultaneous
skin
stringer / clip

Figure 10

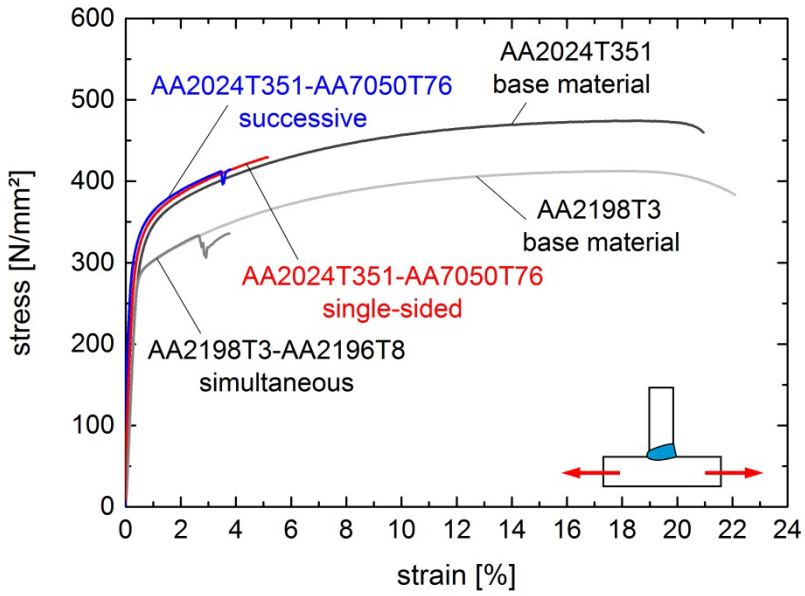
600
500
400
300
200
100
0
stress [N/mm²]
0
2
4
6
8
10
12
14
16
18
20
22
24
strain [%]
AA2024T351
base material
AA2024T351-AA7050T76
successive
AA2198T3
base material
AA2024T351-AA7050T76
single-sided
AA2198T3-AA2196T8
simultaneous

Figure 11

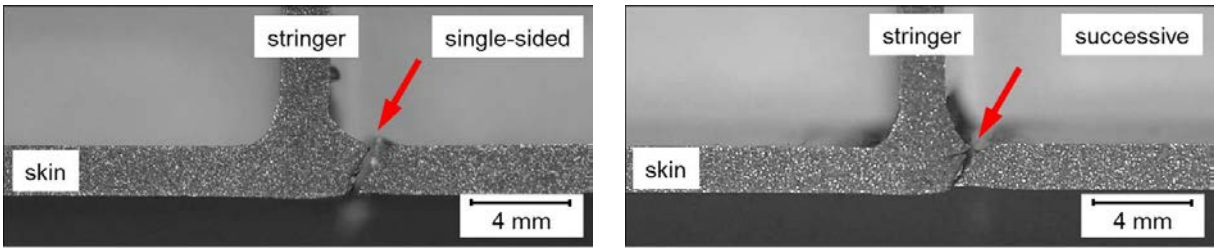
stringer
single-sided
skin
4 mm
stringer
successive
skin
4 mm

(a) (b)

Figure 12

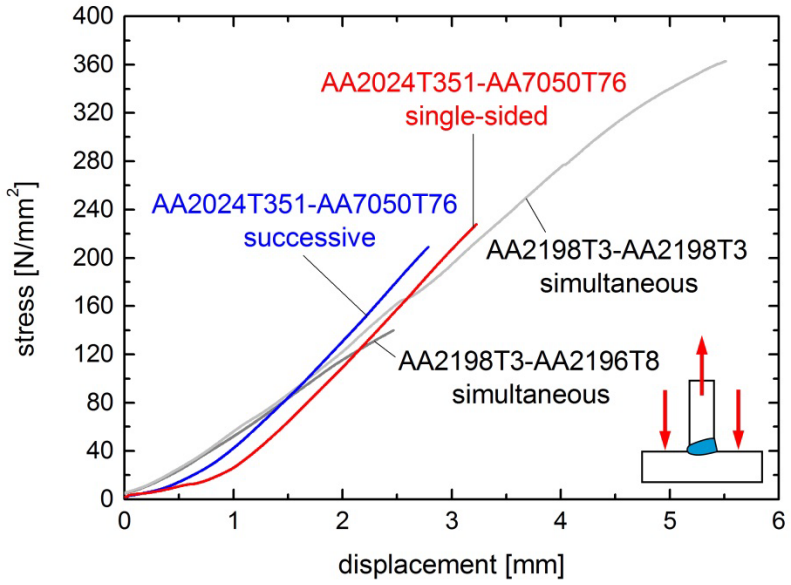
400
360
320
280
240
200
160
120
80
40
0
stress [N/mm²]
0
1
2
3
4
5
6
displacement [mm]
AA2024T351-AA7050T76
single-sided
AA2024T351-AA7050T76
successive
AA2198T3-AA2198T3
simultaneous
AA2198T3-AA2196T8
simultaneous

Figure 13

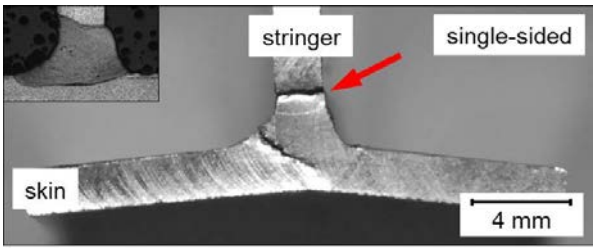
stringer
single-sided
skin
4 mm

(a)

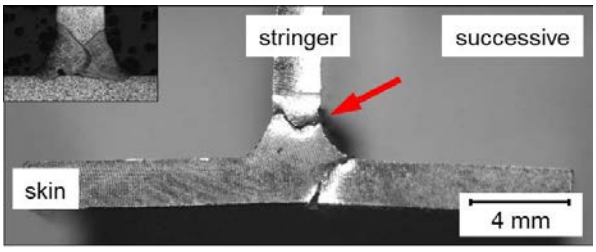
stringer
successive
skin
4 mm

(b)

Table 1

Alloy	Si	Fe	Cu	Mn	Mg	Cr	Zn	Ti	Al
AA2024 (skin)	0.5	0.5	3.8-4.9	0.3-0.9	1.2-1.8	0.1	0.25	0.15	bal.
AA7050 (stringer)	0.12	0.15	2.0-2.6	0.1	1.9-2.6	0.04	5.7-6.7	0.06	bal.
AA4047 (filler wire)	11.0-13.0	0.8	0.3	0.15	0.1	-	0.2	-	bal.

Table 2

Parameter	Unit	single-sided	successive
Laser beam power	kW	8.0	3.5
Incident beam angle	°	15	15
Incident beam position	µm	+0.5	+0.5
Focal position	mm	+8.0	+8.0
Welding speed	m/min	6.0	6.0
Feed rate of filler wire	m/min	8.0	3.0
Flow rate of shielding gas (front/root)	l/min	10/15	20/15

Table 3

Alloy combination (skin - stringer)	Welding method	UTS_W / UTS_{BM} [%]	$A_{f\,W}/A_{f\,BM}$ [%]
AA2024T351 - AA7050T76	single-sided	90.5	24.3
AA2024T351 - AA7050T76	successive	87.3	18.1
AA2198T3 - AA2196T8	simultaneous	81.4	17.2